

# Virtual Plume

Timo Kikas,<sup>+</sup> Hiroshi Ishida,<sup>+</sup> Philip J. W. Roberts,<sup>++</sup> Donald R. Webster,<sup>++</sup> and Jiri Janata\*<sup>+</sup>

<sup>+</sup> School of Chemistry and Biochemistry, Georgia Institute of Technology, Atlanta, GA 30332-0400, USA; e-mail: jiri.janata@chemistry.gatech.edu

<sup>++</sup> Department of Civil & Environmental Engineering, Georgia Institute of Technology, Atlanta, GA 30332, USA

Received: December 10, 1999

Final version: February 9, 2000

## Abstract

A bench-top model of a chemical plume in a turbulent flow, a Virtual Plume, was built to simulate the behavior of a turbulent chemical plume. It is based on an eight-channel FIA/SIA system and an array of eight amperometric sensors. A plug of sample solution was delivered to the sensors after passing through delay and dispersion elements. Adjusting these two elements enabled us to simulate the time-concentration profile at any arbitrary point in the plume. It has been shown that an eight-channel system can simulate an arbitrary sensor array positioned in a turbulent plume. Preliminary correlation of the shape of the peaks obtained in the VP with those recorded using planar laser-induced fluorescence in a turbulent flow shows the value of this approach.

**Keywords:** Virtual/real chemical plume, Turbulent flow, Amperometric sensors, Eight channel system

*Dedicated to Professor Emil Paleček on the Occasion of His 70th Birthday*

## 1. Introduction

The role of environmental analytical chemistry has become increasingly important in recent years. To keep the environment clean, variety of sensors have been developed to monitor pollution. However, elimination of sources of pollution is as important as measurement of pollution levels. Unfortunately it is difficult to locate the source even if the pollutant itself can be detected. The goal of this work is to develop a sensing system capable of tracking the chemical to its source in a turbulent environment. This type of system can also be applied to other similar problems such as searches for unexploded mines, natural resources, etc.

In order to achieve a successful search, the tracking system must be able to deal with a plume of chemical as shown in Figure 1. Molecular diffusion of a chemical substance is generally much slower than the motion of fluid medium (air or

water). It is the turbulence of the flow that mainly determines the distribution of chemicals in the fluid [1]. A chemical substance released from its source trails in the downstream direction, and a number of eddies in the turbulent flow stretch and twist the plume. The result is a complicated, patchy meandering plume as seen in Figure 1. There is no spatially smooth gradient of concentration which might guide a system to the source.

Animals are known to be able to cope with this difficult situation and can trace the smell of food, mates, nest, etc. [2]. Researchers have been studying the mechanisms underlying the search behavior of various animals including moths [3], lobsters [4] and blue crabs [5]. Although they have not yet reached a full understanding, the key points of a successful search have been gradually revealed. Some animals are said to use not only the olfactory sense but also the sense of flow direction to decide their orientation with respect to the source [2, 3]. There is also a lively discussion about the possible information contained in the fine structure of the plume. If a stationary sensor is placed in a turbulent plume, an intermittent signal is obtained. A nonzero signal is obtained when a patch of the plume passes over the sensor, and information about the source location may be encoded into the shape of this signal, for example, the peak values, and intermittency, etc. [1, 6, 7].

Inspired by those findings, several plume tracing systems have been reported both for the searches in air [8–10], and underwater [11]. Those systems have been mostly empirically developed. A new sensing system was built and tested in a wind tunnel, a test room, or a flume, and the performance was optimized with respect to the test conditions.

In this article, a bench-top instrument is proposed to simulate the fundamental behavior of turbulent chemical plumes in water, and the behavior of a sensing array in such plumes. It serves as a “Virtual Plume (VP)”, that can provide information about the behavior of different types of sensors with a variety of chemical stimuli in widely differing fluid dynamic environments. Various sensors, array configurations and signal processing algorithms can then be tested efficiently prior to their testing in a real flume facility.

The VP setup described here is based on the principles of multichannel flow injection analysis (FIA)/sequential injection analysis (SIA) [12, 13] and the array of amperometric chemical

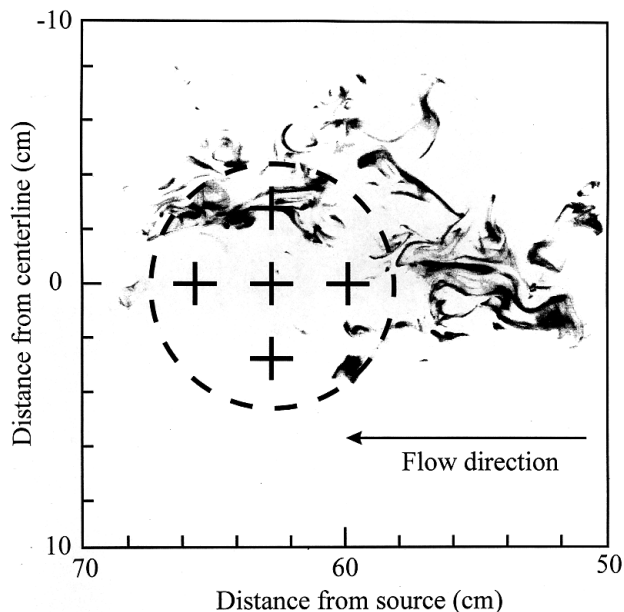


Fig. 1. Image of a chemical plume in a turbulent flow obtained by PLIF. Crosses inside the circle mark positions of the electrodes in the hypothetical sensory array.

sensors [14]. Two fundamental fluid dynamics processes are incorporated into the system: advection of a patch of chemical at the mean flow velocity, and growth of the patch resulting from mixing due to small eddies. Amperometric microsensors are selected for their low detection limit and fast response. The soundness of the system is shown by comparing the sensor signals with data obtained in a real chemical plume measured by planar laser induced fluorescent (PLIF) technique [15, 16] in a turbulent flow.

## 2. Experimental

### 2.1. Amperometric Sensor

Since the main purpose of this work was to characterize the flow system of our bench-top VP setup, the well-defined electrochemical system (platinum microelectrode–hexamine ruthenium(III) chloride) was chosen.

Glass tubes of 3 cm length were cut and their one end was covered with thin platinum film by thermal deposition. 10  $\mu\text{m}$  platinum microwire (Goodfellow, 99.9%) was sealed into the glass tube. The glass tube (Pyrex 7740) had a transformation temperature of 820  $^{\circ}\text{C}$ . The tube has a diameter of about 2 mm at the point of the seal. Microwelder was used to localize the high temperature zone. Contact was made using conducting silver epoxy (EPO-TEK, 417) and silver wire (diameter 0.5 mm) as a connecting wire. The connecting wire was protruding at the end of the capillary tube. The copper cap was attached on top of the platinum-covered end of the glass tube and the end of the connecting wire using conducting epoxy. The platinum electrode was polished flat and used in the flow-system after a cleaning cycle consisting of an ultrasonic bath (2 min, Aquasonic 150HT) and

electrochemical cleaning (1 M  $\text{H}_2\text{SO}_4$ , 20 cycles, from  $-0.4\text{ V}$  to  $+1.0\text{ V}$ , 1 V/s).

A three-electrode electrochemical cell was used in order to prevent current passing through the reference electrode. Silver wire was used as a reference electrode and a stainless steel outlet tube as an auxiliary electrode. A specially designed flow-through cell (see Figure 3b) was used in the experimental setup to ensure identical flow conditions for all the sensors in the VP. Eight sets of electrodes were connected to eight potentiostats (OMNI 90, Cypress Systems, Inc.) and the signals were interfaced to a PC via a DAC interface card (AT-MIO-16XE-10, National Instruments).

### 2.2. Model Electrochemical Reaction

All solutions were made in 0.482 M NaCl solution in order to mimic the high salt concentration in the marine environment and at the same time provide a supporting electrolyte. 2.5 mM solution of hexamine ruthenium trichloride ( $(\text{NH}_3)_6\text{RuCl}_3$ ) was used as the electrochemical marker because the reversible nature of the Ru(III) reduction process assures ideal behavior of amperometric sensors. In the future, ascorbic acid will be used as an electrochemical marker. Ascorbic acid coupled with carbon microelectrodes would give the ability to measure an electrochemical signal in parallel with animal (e.g., crabs and lobsters) tests.

### 2.3. VP Setup

The VP is based on FIA/SIA system and a sensor array of eight amperometric microelectrodes located at the end of eight channels with similar flow conditions but different combination of delay and dispersion elements (see Figure 2). The FIA/SIA

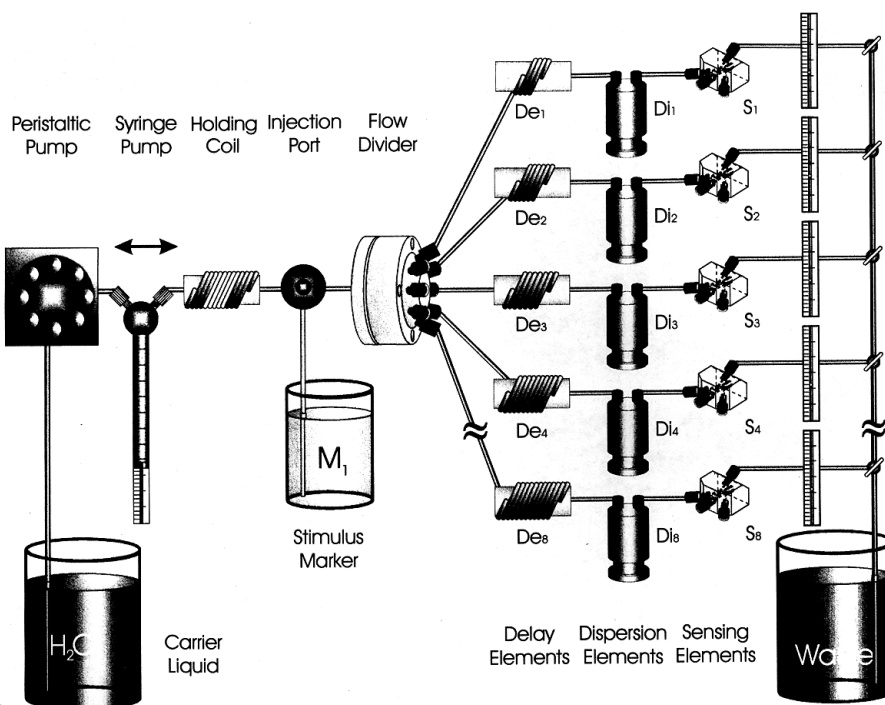


Fig. 2. Schematic of the VP flow system (only five lines of the 8-line system are shown). Where  $\text{De}_n$  is delay element of the  $n$ th line,  $\text{Di}_n$  is dispersion element of the  $n$ th line, and  $\text{S}_n$  is sensing element of the  $n$ th line.

system (FIALab 3000, Alitea USA) has a syringe pump with an usable volume of 5 mL, a peristaltic pump, and a multiport valve. The whole VP system is controlled by the same computer as that used for recording the signals from the sensors.

Either the peristaltic pump or the syringe pump can be used to propel the carrier solution (0.482 M NaCl solution) through the system. The syringe pump creates accurate flow without any pulsation, and is suitable for the single channel experiments described in this article. The peristaltic pump is used when more carrier solution is required, e.g., for the multichannel experiments. The syringe pump was also used to take a sample plug with known volume into the holding coil. This sample plug is then driven through a flow divider, which divides the carrier stream and the sample plug into eight equivalent parts. At the end of each channel, flowmeters with precision valves are used to keep the flow constant in each channel and uniform between all the channels. After passing the flow divider, the divided sample plug is passed through combination of dispersion and delay elements. The former mimic the time lag for a patch of chemical in a real plume to be carried by advection from the source to a certain point, and the latter mimic the dispersion of the patch due to mixing by small eddies. Each channel has a different combination of delay and dispersion elements and therefore mimics different points in the plume. The set of sensing elements at the end of the delay/dispersion line therefore mimics an array of sensors positioned in a real plume.

## 2.4. Individual Elements of the VP Setup

The flow divider was designed to divide the flow into eight identical flows. It consists of a lower body (solution in), an upper body (divided solution fragments out) and Teflon disk between them. The divider outlets are placed radially around the inlet to assure equal flow segments.

The delay elements were designed to provide different retention times for marker plugs while minimizing additional dispersion. Coils of Teflon tubing with inner diameter of 0.5 mm and lengths from 50 cm up to 200 cm were used for this purpose.

The dispersion elements (see Figure 3a) were designed to create considerable additional dispersion without additional delay. The dispersion elements consist of a mixing chamber and movable piston to control the mixing volume of the chamber. A coated magnetic stirring bar driven by rotating magnetic field was used to agitate the solution.

The sensing elements (see Figure 3b) consist of platinum microelectrodes embedded into flow-through cells.

## 2.5. Flow Meters/Controllers

Commercial flow meters/controllers (Accucal flowmeter, Gilmont Instruments) with precision flow control valves (14 turns) were used to measure and equalize flows of different channels. The operating range of the flowmeters is 0.0112–4.92 mL/min.

## 2.6. Plume Data Set

To develop a bench-top analog of a chemical plume, we need to understand its fine spatial and temporal structure. Therefore, the behavior of the VP was compared to measurements of a real

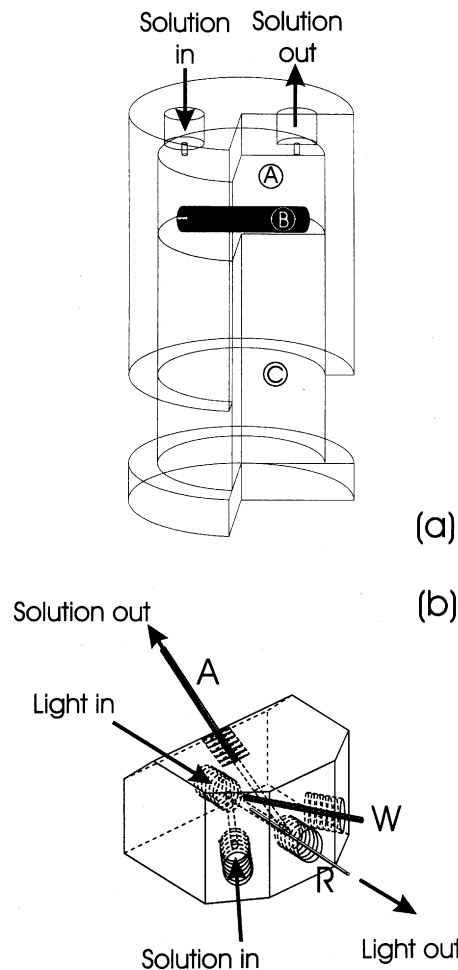


Fig. 3. Schematics of individual elements of the VP flow system. a) Dispersion element, where: A) mixing chamber with changeable volume (0.2–1.5 mL), B) magnetic stirrer bar, C) movable piston. b) Sensing element–flowthrough cell, where: W) working electrode (Pt microelectrode), R) Ag/AgCl reference electrode, A) auxiliary electrode (stainless steel tubing).

plume obtained by the planar laser induced fluorescence (PLIF) measurement technique [15, 16] in a turbulent flow. This non-intrusive, optical measurement is a technique to obtain a sequence of instantaneous, high-resolution spatial concentration fields. Numerical simulations of most turbulent flows are impractical for even the most sophisticated modern super-computers.

A fluorescent dye, Rhodamine 6G, was released isokinetically from a nozzle (4.7 mm ID) into a fully developed open channel water flow in a tilting flume (24.4 m in length  $\times$  1 m in width) [16]. When illuminated with a horizontal laser sheet, the dye emits longer wavelength light with an intensity proportional to its concentration. A digital CCD camera (1024  $\times$  1024 pixels, 8 bit greyscale) captured the emitted light field from above. Typical data sets include over 4000 fields measured at 10 frames per second. After calibration, the raw images were converted to concentration fields.

The sample field shown in Figure 1 spans a 20 cm  $\times$  20 cm field of view, roughly 50 cm downstream from the source. The nozzle and the laser sheet were placed 2.5 cm above the channel bed, and the uniform water depth was 20 cm. The initial concentration of the dye was 120  $\mu\text{g/L}$ , and the exit velocity of the

dye solution from the nozzle matched the mean channel velocity, 5 cm/s.

### 3. Results and Discussion

In order to use electrochemical detection in the VP setup, the mass transport limited region had to be found for the particular electrochemical system. For this purpose, a cyclic voltammogram of hexaaminerutheniumchloride (2.5 mM in 0.482 M NaCl solution) was recorded on the platinum microelectrode against the silver/silverchloride reference electrode in the VP flow system. The cyclic voltammogram was recorded (see Figure 4) at a scan rate of 50 mV/s in a potential window from 0.05 V to  $-0.45$  V. A mass transport limited region was observed in the potential region of  $-0.25$  V to  $-0.4$  V. Based on this result, a working potential of  $-0.3$  V at platinum microelectrodes in the VP flow system was used in all experiments.

In the VP system, a plug of sample solution in the holding coil corresponds to a single patch of chemical in a real plume. When the plug is pushed through the channels with the carrier solution, each sensor shows a single response peak. The peaks showing three repeated measurements with the same sensor but with different delay elements are overlaid in Figure 5a. The amount of sample in a plug was  $50 \mu\text{L}$ , and the flow rate through the channel was  $10 \mu\text{L/s}$ . No dispersion elements were used in these experiments.

As shown in Figure 5a, the peak position was shifted according to the length of the delay element, which corresponds to the distance from the source in a real plume. When a single patch of chemical is carried by the flow over the sensor array, the patch first hits the sensor at the most upstream position, followed by the successive sensors downstream. Therefore, the response curves in Figure 5a can be regarded as the analog of signals from three sensors aligned along the mean flow axis. As expected, the peaks with longer delay elements were slightly more dispersed as they were propelled through the longer paths. However, this additional dispersion is much smaller than that created by the

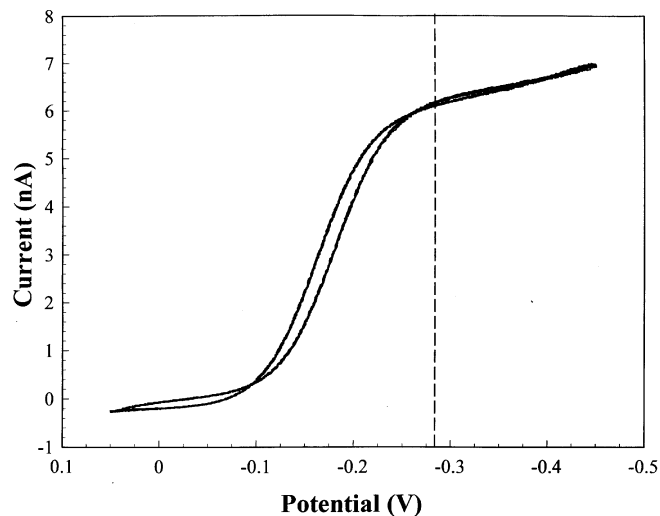


Fig. 4. Cyclic voltammogram of 2.5 mM rutheniumhexamine chloride in the 0.482 M NaCl solution on the platinum working electrode recorded in the VP flow system. The volumetric flow rate was  $10 \mu\text{L/s}$ . A combination of 50 cm delay element and NO dispersion element was used.

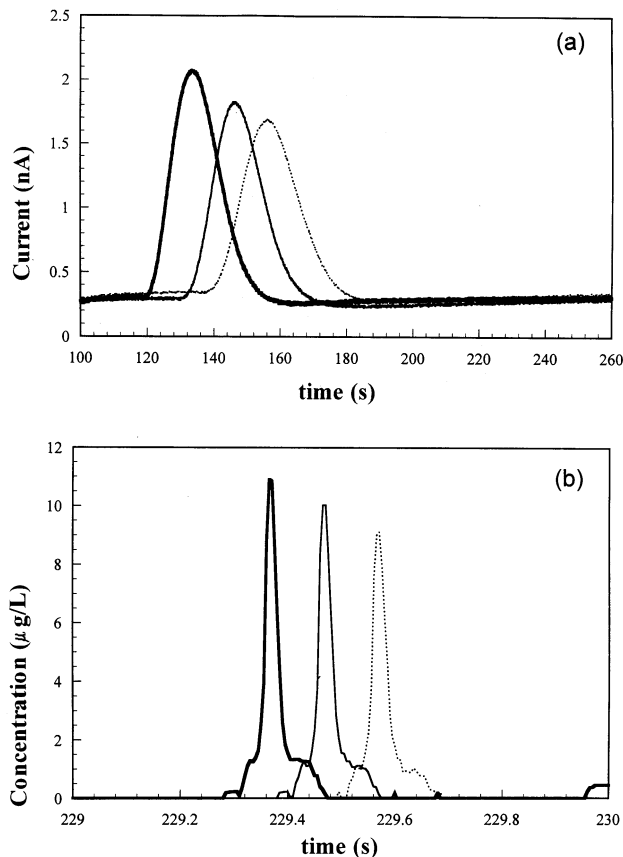


Fig. 5. Effect of delay elements. a) Sensor response with different delay elements. The lengths of the delay lines were 50 cm (thick line), 100 cm (thin line) and 150 cm (dashed line), respectively. b) Concentration profiles in a real plume at three positions on its centerline, spaced 0.5 cm apart. Thick line corresponds to the farthest upstream (59.5 cm downstream from the source) and dashed line to the farthest downstream.

dispersion elements and, therefore, would not be a major problem in achieving an independent control of the delay and the dispersion.

In order to compare the real and VP behavior, time series data of concentration at various positions were extracted from the PLIF data set. The pixel value at a fixed location in the image was first recorded from each frame in the sequence (at 10 samples/s). It was found, however, that this sampling rate was not fast enough to catch every small peak of concentration. Therefore, the concentration data between frames were interpolated. It was assumed that the concentration field was simply advected downstream without change at the mean velocity so that the spatial distribution is frozen between two successive frames. This assumption is reasonable since the velocity fluctuations in this flow were only a few percent of the mean and do not significantly alter the concentration distribution during the short time interval (100 ms) between images. Therefore, the concentration distribution at an instant between images is taken as the weighted average of the previous image shifted downstream and the next image shifted upstream.

Figure 5b shows the concentration profiles interpolated to an equivalent sampling rate of 200 samples/s. Three positions were chosen on the centerline of the plume. The peaks shown in Figure 5b matched the behavior observed in the VP. The highest peak was observed at the most upstream position; the downstream peaks were smaller in magnitude due to turbulent diffusion and

out-of-laser-plane motions of the dye. Although this behavior should be observed in the majority of the samples, the observed peak shapes varied considerably due to the turbulent nature of the flow. Some peaks overlapped with others, and the highest peak was sometimes observed at the most downstream position due to concentration peaks moving into the laser plane from above or below.

Since the flow rate and the plug size was not matched to the flow velocity and the patch size in the real plume, the width of the peak in the VP was not the same order of magnitude as that in a real plume. However, simulation of a real plume is still possible by performing appropriate scaling. Having a bench-top VP is expected to facilitate the research to answer questions such as how fast sensors are needed, what is the optimal spatial arrangement of the sensors, etc.

Figure 6a shows response curves from repeated experiments with different dispersion elements. Although the long delay elements incurred dispersion of the sample plug as shown in Figure 5a, much larger dispersion can be achieved by using the mixing chamber shown in Figure 3a without adding significant delay. The amount of dispersion can be adjusted by changing the volume of the chamber. The larger the chamber, the shorter and the wider peaks were obtained.

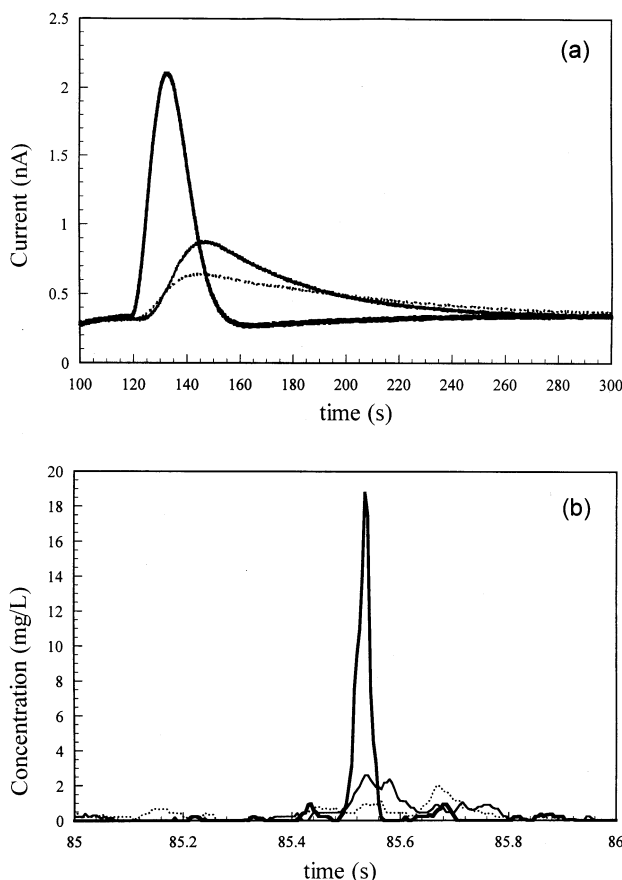


Fig. 6. Effect of dispersion elements. a) Sensor response in VP with different dispersion elements. The volumes of the dispersion elements were 0.0 mL (thick line), 0.4 mL (thin line), and 0.8 mL (dashed line). b) Concentration profile in real plume at three positions placed transversely across the flow direction with the distance between the points of 0.5 cm (thick line corresponds to the centerline response, thin and dashed lines correspond to the responses on each side of centerline).

The effect of the dispersion elements can be related to the effect of small eddies in a turbulent flow. As a patch travels downstream, its size grows and the concentration is reduced since the perimeter of the patch is mixed with the surrounding pure water by turbulent eddies. Therefore, more dispersed concentration peaks can be expected at locations farther away from the source and farther away from the centerline of the plume. Although considerable variation in the peak shapes was observed, statistically significant decreases in the rising slopes of the peaks have been reported at those locations [6, 7]. This change in the peak shape is a possible candidate to decode distance from the source.

Another way to relate Figure 6a to the real plume is shown in Figure 6b. The concentration profiles in the real plume were plotted as in Figure 5b, but the three positions were chosen from the transverse direction with respect to the main flow axis, at 60 cm downstream from the source. The peaks in Figure 6b have similar shapes as in Figure 6a. In the case of Figure 6b, a patch of chemical large enough to cover all three positions arrived, and the center of the patch passed over the center of the three positions. The highest peak at the centerline thus came from the center of the patch, and the smaller peaks came from its diluted perimeter. This arrangement of sensor array may be useful to indicate distance from the plume centerline.

## 4. Conclusions

The soundness of the basic idea of a VP was confirmed by comparing its behavior with concentration profiles observed in a real turbulent plume. Future work will include fine-tuning of various parameters in the VP setup to achieve a better match between the virtual and real plumes. It is also planned to introduce flow modulators into the channels of the flow system. It was found from the plume data set that larger eddies in the turbulent flow cause considerable variation in the shape of the peaks. This process can be simulated by randomly modulating the flow in each channel. The VP system enables us to efficiently try various sensor array configurations in various flow regimes and is expected to facilitate the development of plume tracing systems.

## 5. Acknowledgement

The financial support from DARPA/ONR Project Number: N00014-98-1-0776 is gratefully acknowledged.

## 6. References

- [1] J. Murlis, J.S. Elkinton, R.T. Cardé, *Annu. Rev. Entomol.* **1992**, *37*, 505.
- [2] E.A. Arbas, M.A. Willis, R. Kanzaki, in *Biological Neural Networks in Invertebrate Neuroethology and Robotics* (Eds: R.D. Beer, R.E. Ritzmann, T. McKenna), Academic Press, San Diego **1993**, pp. 159–198.
- [3] T.D. Wyatt, *Nature* **1994**, *369*, 98.
- [4] J. Basil, J. Atema, *Biol. Bull.* **1994**, *187*, 272.
- [5] M.J. Weissburg, R.K. Zimmer-Faust, *Ecology* **1993**, *74*, 1428.
- [6] P.A. Moore, J. Atema, *Biol. Bull.* **1991**, *181*, 408.

- [7] P.A. Moore, M.J. Weissburg, J.M. Parrish, R.K. Zimmer-Faust, G.A. Gerhardt, *J. Chem. Ecol.* **1994**, *20*, 255.
- [8] H. Ishida, K. Suetsugu, T. Nakamoto, T. Moriizumi, *Sens. Actuators A* **1994**, *45*, 153.
- [9] T. Nakamoto, H. Ishida, T. Moriizumi, *Anal. Chem.* **1999**, *4*, 531A.
- [10] R.A. Russell, D. Thiel, R. Devezza, A. Mackay-Sim, *Proc. IEEE Int. Conf. On Robotics and Automation* **1995**, 556.
- [11] T.R. Consi, F. Grasso, D. Mountain, J. Atema, *Biol. Bull.* **1995**, *189*, 231.
- [12] J. Ruzicka, *Analyst* **1998**, *123*, 1.
- [13] J. Ruzicka, L. Scampavia, *Anal. Chem.* **1999**, *4*, 257A.
- [14] K. Potje-Kamloth, J. Janata, M. Josowicz, *Ber. Bunsenges. Phys. Chem.* **1989**, *93*, 1480.
- [15] A.J. Ferrier, D.R. Funk, P.J.W. Roberts, *Dynamics of Atmospheres and Oceans* **1993**, *20*, 155.
- [16] D.R. Webster, P.J.W. Roberts, S. Rahman, L.P. Dasi, *1999 ASCE International Water Resources Engineering Conference* **1999**.